

# Supplementary Material for Accurate Optimization of Weighted Nuclear Norm for Non-Rigid Structure from Motion

José Pedro Iglesias<sup>1</sup>, Carl Olsson<sup>1,2</sup>, and Marcus Valtonen Örnhog<sup>2</sup>

<sup>1</sup> Chalmers University of Technology, Sweden

<sup>2</sup> Lund University, Sweden

## A More details about Algorithm 1 and its implementation

In the main paper we propose the minimization of the objective

$$\min_X a^T \sigma(X) + \|AX - b\|^2 \quad (\text{A.1})$$

through a bilinear parameterization  $X = BC^T$  and using second-order optimization methods such as Levenberg-Marquardt. In Section 5 we provide an overview of the algorithm used, and in this section of the supplementary material we provide more details that were omitted from the main text, in particular how to formulate the problems regarding Low-rank Matrix Recovery (Section 5.2) and Non-rigid Structure Recovery (Section 5.3) using the pOSE error introduced in Section 5.1.

We start by showing how the pOSE term in (A.1) can be written as linear mapping of the elements of  $X$ , resulting in the equivalent objective

$$\min_X a^T \sigma(X) + \|A_X \text{vec}(X) - b_X\|^2. \quad (\text{A.2})$$

The terms  $\ell_{\text{Affine}}$  and  $\ell_{\text{OSE}}$  of the pOSE can be written as

$$\ell_{\text{Affine}} = \|\Gamma_{1:2}X - M\|_F^2 = \|(I \otimes \Gamma_{1:2})\text{vec}(X) - \mathbf{m}\|^2 \quad (\text{A.3})$$

and

$$\ell_{\text{OSE}} = \|\Gamma_{1:2}X - \Gamma_3X \odot M\|_F^2 = \|((I \otimes \Gamma_{1:2}) - \text{diag}(\mathbf{m})(I \otimes \Gamma_3))\text{vec}(X)\|^2, \quad (\text{A.4})$$

where the matrices  $\Gamma_{1:2}, \Gamma_3 \in \mathbb{R}^{2F \times 3F}$  select the desired rows of  $X$  and  $M \in \mathbb{R}^{2F \times P}$  gathers all the 2D observations  $\mathbf{m}_{i,j}$  with  $i = 1, \dots, F$  and  $j = 1, \dots, P$ . We define  $\mathbf{m} = \text{vec}(M)$ . The rows  $2i - 1$  and  $2i$  of  $\Gamma_{1:2}X$  are equal to the rows  $3i - 2$  and  $3i - 1$  of  $X$ , respectively. The rows  $2i - 1$  and  $2i$  of  $\Gamma_3X$  are both equal to the row  $3i$  of  $X$ . To obtain (A.3) and (A.4) we use  $\text{vec}(AXB) = (B^T \otimes A)\text{vec}(X)$ , where  $\otimes$  denotes the Kronecker product.

This allows us to write  $A_X$  and  $b_X$  in (A.2) as

$$A_X = \begin{bmatrix} \sqrt{\eta}(I \otimes \Gamma_{1:2}) \\ \sqrt{1-\eta}((I \otimes \Gamma_{1:2}) - \text{diag}(\mathbf{m})(I \otimes \Gamma_3)) \end{bmatrix}, \quad b_X = \begin{bmatrix} \sqrt{\eta}\mathbf{m} \\ \mathbf{0} \end{bmatrix}. \quad (\text{A.5})$$

We use this as starting point to formulate the problems of Low-rank Matrix Recovery and Non-rigid Structure Recovery, which differ on the way  $X$  in (A.2) is parameterized.

### A.I Low-rank Matrix Recovery with pOSE errors

As seen in Section 5.2, we parameterize  $X = BC^T$ , which results in the objective

$$\sum_{i=1}^p a_i \frac{\|B_i\|^2 + \|C_i\|^2}{2} + \|A_X \text{vec}(BC^T) - b_X\|^2. \quad (\text{A.6})$$

The pOSE term in (A.6) is no longer linear in  $B$  and  $C$ , and in order to apply Levenberg-Marquardt method we linearize it in the neighbourhood of  $B_0$  and  $C_0$  as

$$A_X \text{vec}(BC^T) - b_X \approx \left( A_X \text{vec}(B_0 C_0^T) - b_X \right) + A_B \text{vec}(\delta B) + A_{C^T} \text{vec}(\delta C^T) \quad (\text{A.7})$$

where we define

$$r_{\text{pOSE}} = A_X \text{vec}(B_0 C_0^T) - b_X \quad (\text{A.8})$$

with

$$A_B = A_X(C_0 \otimes I), \quad A_{C^T} = A_X(I \otimes B_0). \quad (\text{A.9})$$

The terms corresponding to the weighted nuclear norm can also be written in a similar fashion since we have

$$\sum_i \frac{a_i}{2} \|B_i\|^2 = \|B \text{diag}(\sqrt{a/2})\|_F^2 = \|(\text{diag}(\sqrt{a/2}) \otimes I) \text{vec}(B)\|^2, \quad (\text{A.10})$$

$$\sum_i \frac{a_i}{2} \|C_i\|^2 = \|\text{diag}(\sqrt{a/2}) C^T\|_F^2 = \|(I \otimes \text{diag}(\sqrt{a/2})) \text{vec}(C^T)\|^2. \quad (\text{A.11})$$

Again, by considering the deviations from the current estimations,  $B = B_0 + \delta B$  and  $C = C_0 + \delta C$ , we end up with

$$A_{\text{regB}} = \text{diag}(\sqrt{a/2}) \otimes I, \quad r_{\text{regB}} = (\text{diag}(\sqrt{a/2}) \otimes I) \text{vec}(B_0), \quad (\text{A.12})$$

$$A_{\text{regC}} = I \otimes \text{diag}(\sqrt{a/2}), \quad r_{\text{regC}} = (I \otimes \text{diag}(\sqrt{a/2})) \text{vec}(C_0^T). \quad (\text{A.13})$$

As so, we can compute the residuals and jacobian in Algorithm 1 for the Low-rank Matrix Recovery problem as

$$J = \begin{bmatrix} A_B & A_{C^T} \\ A_{\text{regB}} & \mathbf{0} \\ \mathbf{0} & A_{\text{regC}} \end{bmatrix}, \quad r_a = \mathcal{A}_a(B_0 C_0^T) + b_a = \begin{bmatrix} r_{\text{pOSE}} \\ r_{\text{regB}} \\ r_{\text{regC}} \end{bmatrix}. \quad (\text{A.14})$$

### A.II Non-Rigid Structure Recovery

When considering the Non-rigid Structure Recovery problem, we use the parameterization  $X = Rg(BC^T) + t\mathbb{1}^T$ . This also results in a non-linear pOSE term in terms of  $B$  and  $C$ , and its linearization around  $B_0$ ,  $C_0$  and  $t_0$  are obtained as

$$\begin{aligned} A_X \text{vec}(Rg(BC^T) + t\mathbb{1}^T) - b_X &\approx \\ &\approx \left( A_X \text{vec}(Rg(B_0 C_0^T) + t_0 \mathbb{1}^T) - b_X \right) + A_B \text{vec}(\delta B) + A_{C^T} \text{vec}(\delta C^T) + A_t \delta t \end{aligned} \quad (\text{A.15})$$

where we now define

$$r_{\text{pOSE}} = A_X \text{vec}(Rg(B_0 C_0^T) + t_0 \mathbb{1}^T) - b_X \quad (\text{A.16})$$

with

$$A_B = A_X(I \otimes R)\Gamma_g(C_0 \otimes I), \quad A_{C^T} = A_X(I \otimes R)\Gamma_g(I \otimes B_0), \quad A_t = A_X(\mathbb{1} \otimes I), \quad (\text{A.17})$$

where  $\Gamma_g$  maps the elements from  $BC^T$  to  $g(BC^T)$  such that

$$\text{vec}\left(g(BC^T)\right) = \Gamma_g \text{vec}\left(BC^T\right). \quad (\text{A.18})$$

Since the weights  $a$  are applied to the singular values of  $BC^T$ , the weighted nuclear norm terms can be written as (A.12) and (A.13), similarly to the Low-rank Matrix Recovery problem. The residuals and jacobian in Algorithm 1 for the Non-rigid Structure Recovery problem can be computed as

$$J = \begin{bmatrix} A_B & A_{C^T} & A_t \\ A_{\text{regB}} & \mathbf{0} & \mathbf{0} \\ \mathbf{0} & A_{\text{regC}} & \mathbf{0} \end{bmatrix}, \quad r_a = \mathcal{A}_a(B_0 C_0^T) + b_a = \begin{bmatrix} r_{\text{pOSE}} \\ r_{\text{regB}} \\ r_{\text{regC}} \end{bmatrix}, \quad (\text{A.19})$$

and the translation is also added to the auxiliary variable  $z$  in Algorithm 1, i.e.,  $z = [\text{vec}(B); \text{vec}(C^T); t]$ .

## B Results on Back, Heart and Paper Datasets

In Figure C.1 we show an example of the reprojection errors obtained for the Back, Heart and Paper datasets in Section 5.2, for the weighted nuclear norm regularization and  $\eta = 0.05$  (near perspective). Even though the qualitative difference between the methods is not visible (note the y-axis scale on the plots in Figure 1), the second-order method was still able to obtain a lower loss than all the first-order methods.

## C Results on NRSfM Challenge Datasets

In this section we provide all results obtained with the weighted nuclear norm for the perspective camera model of the NRSfM Challenge datasets. These include the the log-losses (Table C.1) and 3D reconstruction errors (Table C.2) for the ADMM and our method, in each of the six sequences (Circle, Flyby, Line, Semi-circle, Tricky, Zigzag) of the five datasets. Recall that the values in Tables 1 and 2 in the main text correspond to the average over the six sequences, for each dataset. In Figures C.2 and C.3 we also show the qualitative comparison between the 3D reconstruction obtained with the two methods and the provided 3D ground-truth structure, for each sequence.

Note that our method is always able to obtain a lower loss compared to the ADMM, and the 3D reconstruction is always as good or much better (see the cases of Ballon-Semi-circle, Balloon-Tricky, Paper-Tricky, and Stretch-Flyby). The only exception was the sequence Tearing-Zigzag, where a lower loss actually resulted in a worse 3D reconstruction, which might be explained by incorrect modeling ( $K = 2$  might be too low for this sequence).

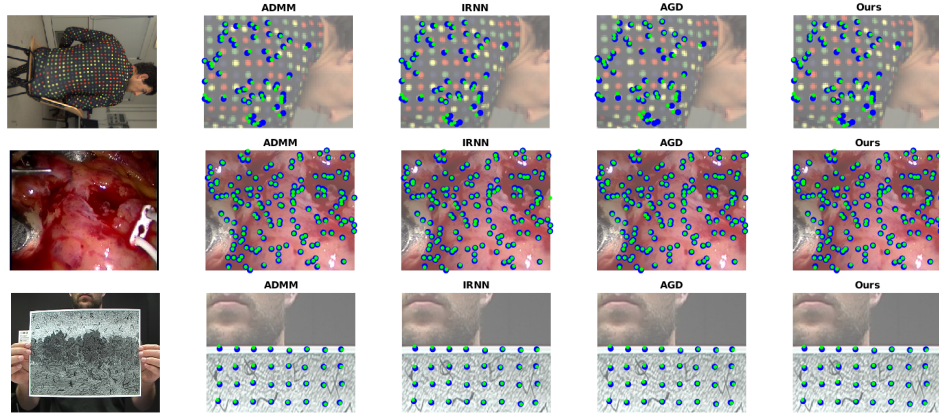


Fig. C.1: Comparison between reprojections (green) and 2D measurements (blue) obtained in Section 5.2 for Back (top), Heart (middle), and Paper (bottom) datasets.

Table C.1: Log-loss on each for all sequences of the perspective datasets.

Method \ Sequence		Circle	Flyby	Line	Semi-circle	Tricky	Zigzag
Articulated	ADMM-WNN	-1.822	-2.849	-3.797	-3.405	-3.009	-2.517
	Ours-WNN	<b>-1.825</b>	<b>-2.853</b>	<b>-3.845</b>	<b>-3.408</b>	<b>-3.030</b>	<b>-2.753</b>
Balloon	ADMM-WNN	-2.232	-2.977	-3.130	-2.607	-2.380	-3.834
	Ours-WNN	<b>-2.465</b>	<b>-3.325</b>	<b>-3.096</b>	<b>-2.949</b>	<b>-2.934</b>	<b>-4.037</b>
Paper	ADMM-WNN	-1.451	-3.037	-3.822	-3.171	-3.112	-3.473
	Ours-WNN	<b>-2.107</b>	<b>-3.037</b>	<b>-3.823</b>	<b>-3.171</b>	<b>-3.809</b>	<b>-3.498</b>
Stretch	ADMM-WNN	-2.267	-2.253	-3.629	-2.722	-3.574	-4.542
	Ours-WNN	<b>-2.275</b>	<b>-3.153</b>	<b>-3.846</b>	<b>-2.724</b>	<b>-3.578</b>	<b>-4.546</b>
Tearing	ADMM-WNN	-1.834	-1.154	-3.302	-1.888	-3.504	-1.612
	Ours-WNN	<b>-2.184</b>	<b>-1.662</b>	<b>-3.302</b>	<b>-2.067</b>	<b>-3.521</b>	<b>-2.017</b>

Table C.2: 3D reconstruction error, in millimeters, on each for all sequences of the perspective datasets relatively to the provided ground-truth structure.

Method \ Sequence		Circle	Flyby	Line	Semi-circle	Tricky	Zigzag
Articulated	ADMM-WNN	15.69	<b>9.52</b>	13.33	16.49	<b>27.77</b>	26.65
	Ours-WNN	<b>13.84</b>	9.67	<b>12.35</b>	<b>14.32</b>	32.49	<b>16.52</b>
Balloon	ADMM-WNN	3.56	<b>2.64</b>	<b>4.73</b>	16.06	24.46	2.23
	Ours-WNN	<b>2.07</b>	2.92	4.78	<b>5.48</b>	<b>20.19</b>	<b>2.19</b>
Paper	ADMM-WNN	8.62	<b>4.71</b>	<b>6.71</b>	6.12	30.45	<b>4.22</b>
	Ours-WNN	<b>1.98</b>	4.75	7.06	<b>6.02</b>	<b>9.80</b>	4.45
Stretch	ADMM-WNN	<b>2.59</b>	16.86	<b>4.78</b>	5.68	15.65	<b>2.80</b>
	Ours-WNN	2.69	<b>2.85</b>	6.74	<b>5.58</b>	<b>14.93</b>	2.84
Tearing	ADMM-WNN	5.10	10.94	<b>8.93</b>	5.05	18.57	<b>7.09</b>
	Ours-WNN	<b>4.25</b>	<b>7.15</b>	9.17	<b>4.87</b>	<b>16.98</b>	8.12

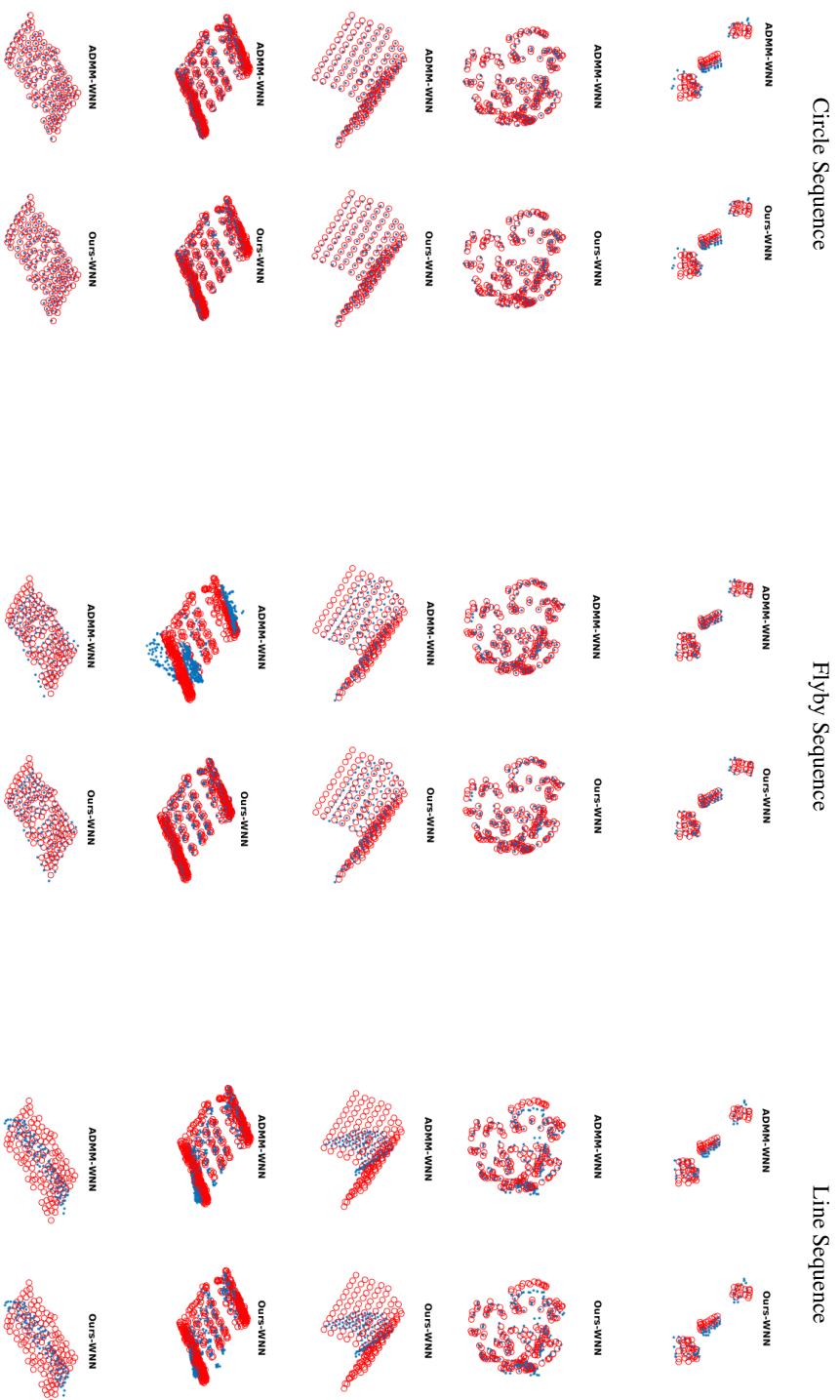


Fig. C.2: Comparison between the estimated (blue) and provided (red) 3D structure for the sequences Circle, Flyby and Line.

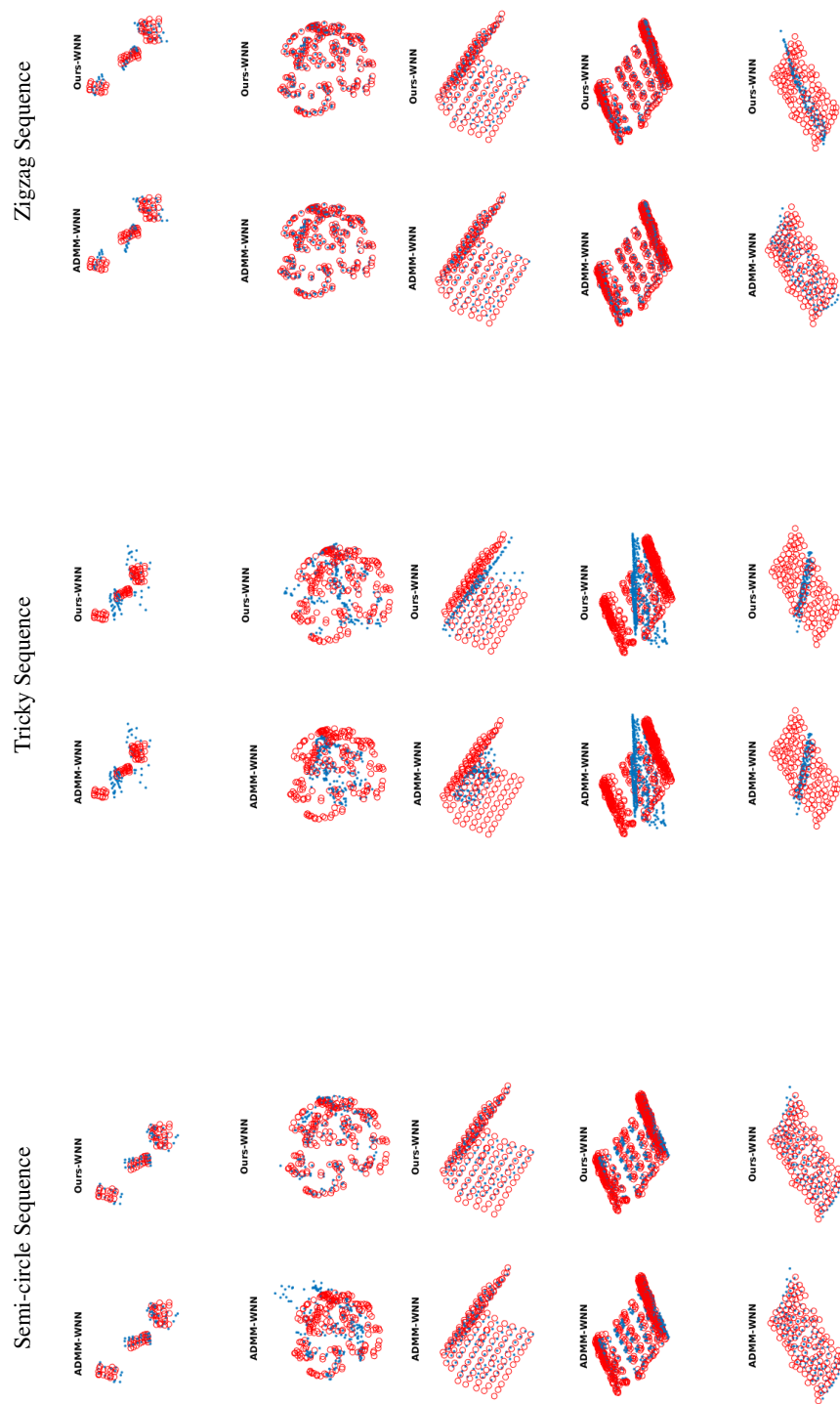


Fig. C.3: Comparison between the estimated (blue) and provided (red) 3D structure for the sequences Semi-circle, Tricky and Zigzag.